crystallization communications

Two-step counterdiffusion protocol for the crystallization of haemoglobin II from *Lucina pectinata* in the pH range 4–9

Carlos A. Nieves-Marrero,[a]
Carlos R. Ruiz-Martínez,[a]
Rafael A. Estremera-Andújar,[a]
Luis A. González-Ramírez,[b]
Juan López-Garriga[a] and
José A. Gavira[b]*

[a]Chemistry Department, PO Box 9019, University of Puerto Rico, Mayagüez Campus, Mayagüez, PR 00681, Puerto Rico, and [b]Laboratorio de Estudios Cristalográficos, Instituto Andaluz de Ciencias de la Tierra, CSIC-Universidad de Granada, Edificio López Neyra, PTCS, Avenida del Conocimiento, s/n 18100 Armilla, Granada, Spain

Correspondence e-mail: jgavira@ugr.es

Lucina pectinata haemoglobin II (HbII) transports oxygen in the presence of H_2S to the symbiotic system in this bivalve mollusc. The composition of the haem pocket at the distal site includes TyrB10 and GlnE7, which are very common in other haem proteins. Obtaining crystals of oxyHbII at various pH values is required in order to elucidate the changes in the conformations of TyrB10 and GlnE7 and structural scenarios induced by changes in pH. Here, the growth of crystals of oxyHbII using the capillary counterdiffusion (CCD) technique at various pH values using a two-step protocol is reported. In the first step, a mini-screen was used to validate sodium formate as the best precipitating reagent for the growth of oxyHbII crystals. The second step, a pH screen typically used for optimization, was used to produce crystals in the pH range 4–9. Very well faceted prismatic ruby-red crystals were obtained at all pH values. X-ray data sets were acquired using synchrotron radiation of wavelength 0.886 Å (for the crystals obtained at pH 5) and 0.908 Å (for those obtained at pH 4, 8 and 9) to maximum resolutions of 3.30, 1.95, 1.85 and 2.00 Å for the crystals obtained at pH 4, 5, 8 and 9, respectively. All of the crystals were isomorphous and belonged to space group $P4_22_12$.

1. Introduction

The clam *Lucina pectinata* was collected from the sulfide-rich muddy mangrove areas of the south-west coast of Puerto Rico (Kraus & Wittenberg, 1990). It contains three different haemoglobins (HbI, HbII and HbIII) and a cysteine-rich (p-Cys) protein (Read, 1965). HbII is known to be an oxygen-reactive haemoglobin that provides oxygen, in the presence of H_2S, to the gills and for bacterial symbiosis (Vinogradov *et al.*, 1993). This haemoprotein is composed of 150 amino-acid residues and has a molecular weight of 16 128 Da (Hockenhull-Johnson *et al.*, 1991). cDNA amino-acid sequence analysis proposed the following HbII haem-pocket composition at the distal site: Tyr(30)B10, Gln(65)E7, Phe(69)E11 and Phe(44)CD1 (Torres-Mercado *et al.*, 2003). The crystallographic model of HbII confirmed the amino-acid composition of the pocket (Gavira *et al.*, 2008). The first HbII crystallization condition was obtained using the hanging-drop vapour-diffusion method. The crystallization condition employed was 8% saturated ammonium sulfate solution and 50 m*M* Tris–HCl pH 7, using protein at 1.9 m*M* in 50 m*M* phosphate buffer pH 7.5 and 0.05 m*M* EDTA (Doyle *et al.*, 1994; Kemling *et al.*, 1991). Another crystallization condition was obtained in a 0.2 mm capillary containing 0.1%(*w/v*) agarose using a lyophilized HbII sample dissolved in 50 m*M* bis-tris propane buffer pH 7 with 0.5 m*M* EDTA. The protein concentration was approximately 30 mg ml^{-1}; the crystal had dimensions of $0.20 \times 0.05 \times 0.05$ mm and belonged to the primitive tetragonal space group $P4_22_12$. Diffraction data were collected to a resolution of 1.93 Å using synchrotron radiation of wavelength 0.97 Å (Gavira *et al.*, 2006).

The structural findings showed a dimeric association in the asymmetric unit in which the O_2 ligand was anchored at 110° to the haem group through hydrogen bonds to TyrB10 and GlnE7; the haem pocket was smaller compared with that of HbI (Gavira *et al.*, 2008). The suggested model for ligand stabilization in HbII is based on the hydrogen-bond network between TyrB10 and GlnE7 at the haem

distal site, but additional data are necessary in order to infer the ligand-selection mechanism. Very similar hydrogen-bonding networks are present in the truncated haemoglobins (trHbs) found in organisms such as *Ascaris suum* (Hb$_{Asc}$) and *Mycobacterium tuberculosis* (trHbO and trHbN). TyrB10 and GlnE7 also proved to be responsible for the oxidative stability of the haem towards H_2O_2 and the distal control of NO binding in HbII from *L. pectinata*. Finally, each of these haemoglobins has a specific behaviour and function in their respective organism and have the TyrB10 and GlnE7 residues in common, which apparently play an important role in the ligand-discrimination mechanism (De Baere *et al.*, 1994; Mukai *et al.*, 2002; Ouellet *et al.*, 2003; De Jesús-Bonilla *et al.*, 2007). Disruption of the hydrogen-bonding network in the TyrB10 and GlnE7 haem moiety by conformational changes may create the relevant driving force to understand the oxygen-affinity behaviour of HbII and other proteins with similar distal haem centres. This is supported by spectrophotometric acid–base titration of HbII and HbI (PheB10Tyr) mutants, which showed the appearance of a 603 nm band as a function of pH (De Jesús-Bonilla *et al.*, 2006). The effect of pH on the ligand and on the hydroxyl group of the tyrosine could play a fundamental role as a stabilization force inside the haem moiety (Peterson *et al.*, 1997).

Several crystallographic studies have been conducted to investigate specific conformational changes in proteins as a function of pH. In the case of ribonuclease A, for instance, a structural change was revealed based on the deprotonation of Lys41 in the pH range 8.0–8.8. At these pH values it was also suggested that Lys7 and Arg10 could stabilize the catalytically active conformation of Lys41 (Berisio *et al.*, 2002). In haem proteins the influence of pH has been reported for carbonmonoxymyoglobin (MbCO), showing that at pH 4 HisE7 swings out of the haem pocket. This movement pushes out ArgCD3, leaving the pocket completely open and keeping HisE7 stabilized by a hydrogen-bond network (Yang & Phillips, 1996). Similar structural studies have been performed on other haem proteins such as dihaem cytochrome *c* peroxidase from *Pseudomonas nautica* (Dias *et al.*, 2002), horse methaemoglobin (Robinson *et al.*, 2003) and haemoglobin from *Trematomus bernacchii* (Mazzarella *et al.*, 2006) among others. Following these studies, we expect that crystallographic structural models of oxyHbII at different pH values will provide specific information on the disruption of the hydrogen-bonding network in the TyrB10 and GlnE7 haem moiety that may induce changes in the oxygen-selection mechanism.

In this work, we describe the use of the two-step counterdiffusion protocol with prefilled GCB kits (Triana Science and Technology), which are typically used in our laboratory to improved protein crystal quality, to grow oxyHbII crystals at pH values in the range 4–9.

2. Materials and methods

2.1. Protein isolation, purification and concentration

L. pectinata clams were collected and HbII was isolated and purified from a raw extract using modifications (Ruiz-Martínez *et al.*, 2009) of previously published protocols (Kraus & Wittenberg, 1990). Summarizing the steps, the HbII–III complex was isolated and purified from the raw extract using a fast protein liquid-chromatography system (FPLC) with a HiLoad 26/60 Superdex 200 grade (ÄKTA; Amersham Bioscience) size-exclusion chromatography (SEC) column. HbII and HbIII were separated from the HbII–III complex by one step of anion-exchange chromatography using a HiPrep 16/10 QFF column coupled with a HiTrap QFF (5 ml) precolumn. The oxyHbII complex (referrred to in the following as HbI) was obtained by bubbling oxygen at 101.3 kPa and was monitored by its characteristic UV–Vis spectrum (Kraus & Wittenberg, 1990). Finally, the sample was concentrated in water using an Amicon ultrafiltration concentrator system with a YM-10 membrane. The final concentration of HbII in water was determined using the reported Soret and Q band values (Kraus & Wittenberg, 1990) and was adjusted to 30 mg ml^{-1} for the crystallization experiments.

2.2. Crystallization by the two-step counterdiffusion technique

The two-step crystallization procedure normally used with the counterdiffusion method (Garcia-Ruiz, 2003) for initial screening and crystal improvement was followed. In the first step, initial crystallization conditions are screened using the 24-condition Crystallization Screening Kit (GCB-CSK; Triana Science and Technology) adapted from the mini-screen described by Kimber & Vallee (2003). Less than 10 µl of protein solution is sufficient to set up a whole screen. The second step, crystal quality and/or size improvement, is investigated
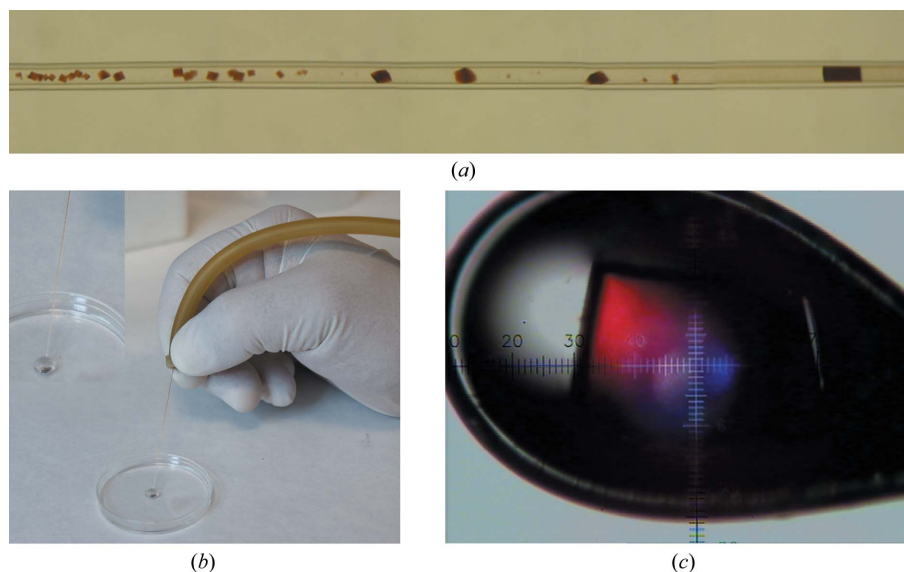

Figure 1
(*a*) OxyHbII counterdiffusion behaviour in a 0.2 mm capillary. (*b*) The crystals grown from the GCB capillaries were extracted and equilibrated in 50 µl cryoprotectant solution. (*c*) A crystal of oxyHbII grown at pH 8.0, mounted on a nylon loop and flash-cooled in a 100 K liquid-nitrogen jetstream.

by changing the pH. This screen can be performed using the GCB-Domino Crystallization Kit (GCB-D; Triana Science and Technology) with selected precipitant agents at pH values ranging from 4 to 9. Capillaries of 0.2 mm inner diameter can be used in the improvement step, with a consumption of approximately 5 µl protein solution per screen (six capillaries).

For the crystallization of oxyHbII, both steps were followed. Precipitants selected from the initial screen, 5 M sodium formate (KIT-SF-49), 3 M ammonium sulfate (KIT-AS-49) and 1.5 M lithium sulfate (KIT-LS-49), were used to produce crystals in the pH range 4–9. All of the counterdiffusion experiments were set up using 0.2 and 0.3 mm inner diameter glass capillaries. The viscosity of the protein solutions used to fill the capillaries of 0.3 mm inner diameter was increased with 0.1%(w/v) agarose gel in order to avoid convection (Gavira et al., 2006; Ruiz-Martínez et al., 2009). All screenings and crystallization experiments were carried out at 293 K. Fig. 1(a) shows the typical crystal-distribution pattern obtained with the counterdiffusion technique.

2.3. Data collection

X-ray diffraction data sets were collected on beamline BM-16 at the European Synchrotron Radiation Facility (ESRF). Data acqui-sition was performed using a wavelength of 0.886 Å for crystals grown at pH 5 and of 0.908 Å for crystals grown at pH 4, 8 and 9 with an ADSC Quantum 4R detector. Crystals were selected by visual inspection and extracted from the capillary into 50 µl of an isotonic solution containing 15%(v/v) glycerol as a cryoprotectant solution (Fig. 1b). As described previously, if the crystals adhered to the capillary wall then they were gently removed with a cat whisker (Ruiz-Martínez et al., 2009). After a minimum of 30 s, one crystal was selected with a loop and flash-cooled in a 100 K liquid-nitrogen jet-stream produced by an Oxford 600 CryoSystem (Fig. 1c). All the collected data sets were indexed, integrated and scaled using the HKL-2000 suite (Otwinowski & Minor, 1997).

3. Results and discussion

Initial crystallization conditions were screened using the 24-condition Crystallization Screening Kit (GCB-CSK; Triana Science and Technology) adapted from the mini-screen described by Kimber & Vallee (2003). As previously observed during crystallization experiments of HbII using vapour diffusion (Kemling et al., 1991; Doyle et al., 1994) and counterdiffusion techniques (Gavira et al., 2006) and in the crystallization of the oxy and cyano forms of the HbII–III complex
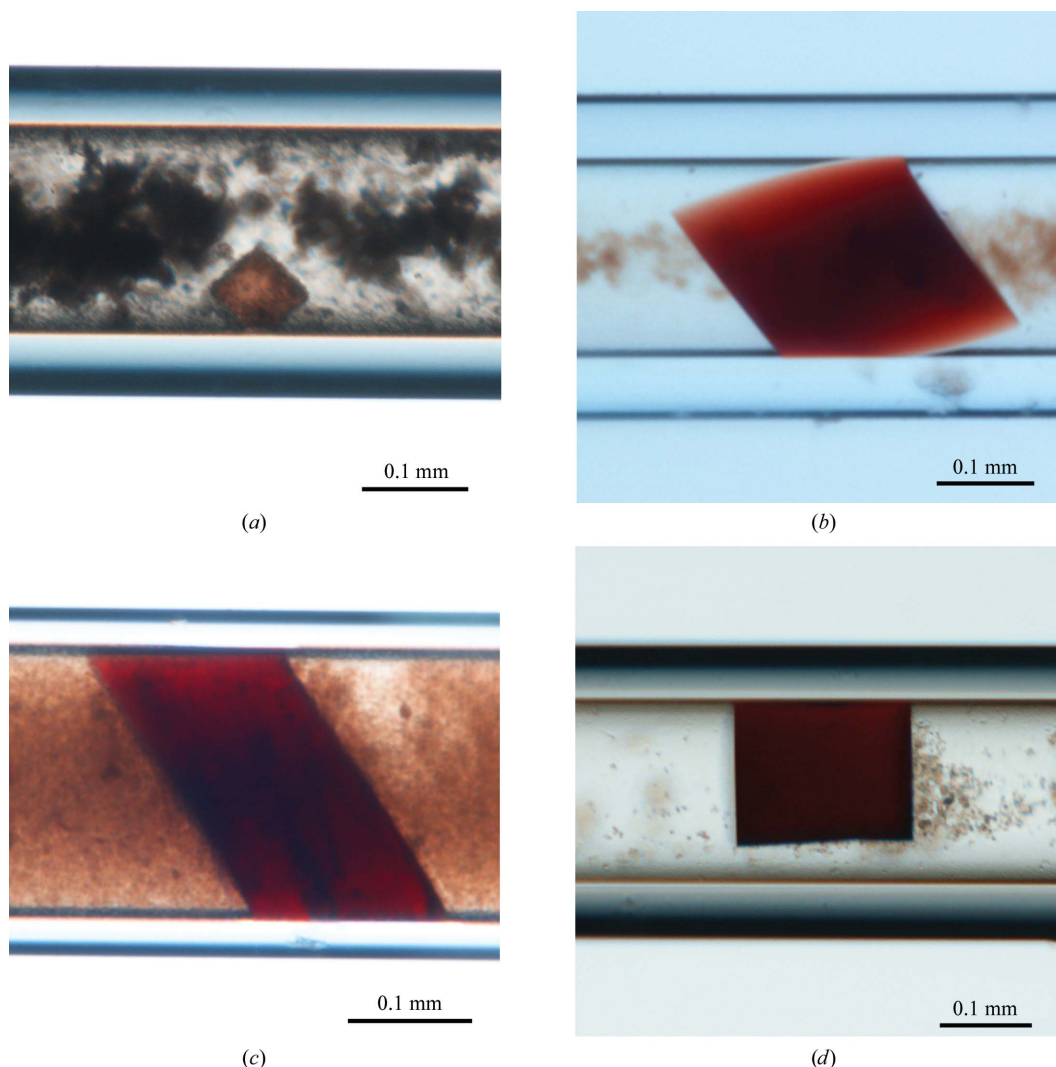

(a)	(b)
0.1 mm	0.1 mm

(c)	(d)
0.1 mm	0.1 mm

Figure 2
Representative crystals of oxyHbII obtained in sodium formate at (a) pH 4, (b) pH 5, (c) pH 8 and (d) pH 9.

Table 1
Summary of X-ray data and statistics for oxyHbII crystals precipitated with sodium formate at different pH values.

Values in parentheses are for the highest resolution shell.

	pH 4.0	pH 5.0	pH 8.0	pH 9.0
Wavelength (Å)	0.908	0.886	0.908	0.908
Distance (mm)	304	183	184	184
Exposure time (s)	35	10.89	10	10
Oscillation angle (°)	1	0.5	0.5	0.5
No. of frames	138	300	219	154
Space group	$P4_22_12$	$P4_22_12$	$P4_22_12$	$P4_22_12$
Unit-cell parameters (Å)	$a = b = 72.24, c = 146.29$	$a = b = 73.97, c = 153.19$	$a = b = 74.71, c = 152.65$	$a = b = 75.92, c = 153.13$
Resolution range (Å)	20.0–3.30 (3.42–3.30)	20.0–1.95 (2.02–1.95)	20.0–1.85 (1.92–1.85)	20.0–2.00 (2.07–2.00)
Observed reflections	49134	331004	317299	126200
Independent reflections	6617	31837	37149	29505
Data completeness (%)	97.1 (95.2)	99.9 (100.0)	98.4 (100)	95.5 (98.1)
R_{merge}† (%)	14.5 (49.2)	13.8 (42.2)	6.0 (49.1)	13.0 (51.2)
Average $I/\sigma(I)$	13.3 (3.8)	16.0 (6.4)	25.9 (4.34)	7.8 (1.9)
Redundancy	7.4 (7.0)	10.4 (9.5)	8.5 (8.7)	4.3 (4.0)
Mosaicity	1.6	0.5	0.9	1.2
Molecules per ASU	2	2	2	2
Matthews coefficient (Å³ Da⁻¹)	2.96	3.25	3.30	3.28
Solvent content (%)	58.40	62.11	62.74	62.55

† $R_{merge} = \sum_{hkl} \sum_i |I_i(hkl) - \langle I(hkl) \rangle| / \sum_{hkl} \sum_i I_i(hkl)$, where $I_i(hkl)$ is the ith measurement of reflection hkl and $\langle I(hkl) \rangle$ is the weighted mean of all measurements.

(Ruiz-Martínez *et al.*, 2009) a large number of hits were obtained (11 conditions), but only those crystals grown in the presence of sulfate or formate were of good optical quality. The specific formulations of each crystallization condition, as reported in the GCB-CSK screening kit, are as follows: (i) 2.0 *M* ammonium sulfate, 0.1 *M* HEPES pH 7.5, 4% PEG 400 (condition No. 5), (ii) 2.0 *M* ammonium sulfate, 0.1 *M* Tris–HCl pH 8.0 (condition No. 7), (iii) 2.0 *M* lithium sulfate, 0.1 *M* HEPES–NaOH pH 7.0 (condition No. 17) and (iv) 6.0 *M* sodium formate (condition No. 21). Only three conditions were selected to produce oxyHbII crystals in the pH range 4–9 using the crystal-improvement kits from Triana Science and Technology: (i) KIT-SF-49 (5.0 *M* sodium formate), (ii) KIT-LS-49 (2.0 *M* lithium sulfate) and (iii) KIT-AS-49 (3.0 *M* ammonium sulfate). Of these, only the kit containing 5 *M* sodium formate (KIT-SF-49) produced crystals that
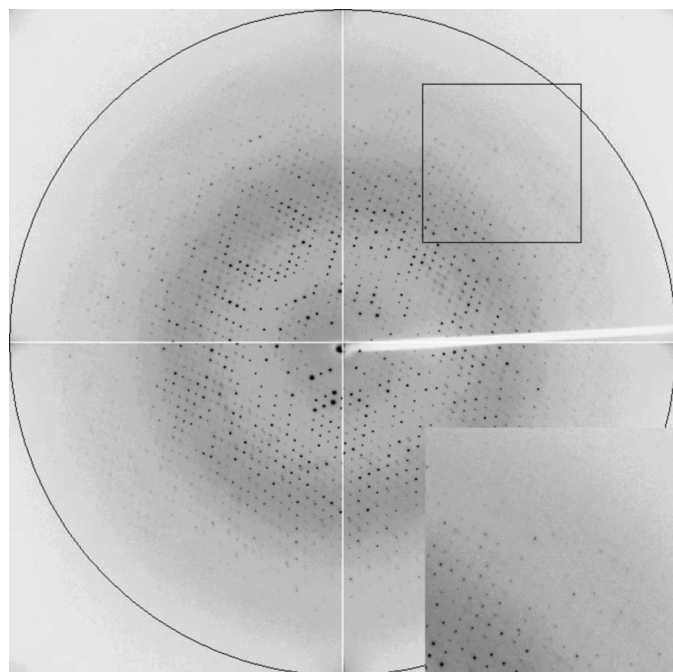
were suitable for X-ray analysis in the whole pH range independent of the capillary diameter and the presence of agarose gel. These results suggested that the conformational changes observed as a function of the pH (De Jesús-Bonilla *et al.*, 2006) do not completely disrupt the crystal contacts. Fig. 2 shows examples of the ruby-red prismatic crystals obtained at pH 4, 5, 8 and 9. All crystals belonged to the tetragonal space group $P4_22_12$, with unit-cell parameters similar to those previously reported for HbII (Gavira *et al.*, 2006), HbIII (Kemling *et al.*, 1991) and the HbII–III complex (Ruiz-Martínez *et al.*, 2009) and therefore with two monomers in the asymmetric unit. Table 1 shows the complete data-collection protocols and statistics for HbII samples.

Crystal quality was found to be pH-dependent. The worst diffracting crystals were grown at pH 4, with the best tested crystal diffracting X-rays to a maximum resolution of 3.30 Å, and presented the smallest unit cell. Meanwhile, the crystals obtained at pH 5 and 9 diffracted X-rays to resolutions of 1.95 and 2.0 Å, respectively. The crystal grown at pH 8 in 0.3 mm capillaries in the presence of agarose had the highest quality, with a resolution limit of 1.85 Å (Fig. 3). The clean HbII structural model (PDB code 2olp, chain *A*; Gavira *et al.*, 2008) was used to search for a molecular-replacement solution using the *MOLREP* program (Vagin & Teplyakov, 1997). The four structures are currently undergoing refinement using *REFMAC*5 (Murshudov *et al.*, 1997) from the *CCP*4 suite (Collaborative Computational Project, Number 4, 1994).

4. Conclusions

The efficiency of the two-step counterdiffusion crystallization procedure was confirmed for the initial screening and crystal improvement of oxyHbII crystals in the pH range 4–9. The crystals grown at pH 4.0 diffracted to the lowest resolution. This behaviour could be attributed either to the protonation of residues involved in crystal contacts, to dramatic conformational changes or to a combination of both. However, the crystals grown at pH 5, 8 and 9 had excellent diffraction patterns to resolutions of 1.95, 1.85 and 2.00 Å, respectively, allowing complete structural comparison as a function of pH.

Figure 3
X-ray diffraction frame of oxyHbII obtained at pH 8 by the counterdiffusion method.

The authors wish to thank the staff of BM16 (ESRF) for their assistance during data collection. We gratefully acknowledge

crystallization communications

References

Berisio, R., Sica, F., Lamzin, V. S., Wilson, K. S., Zagari, A. & Mazzarella, L. (2002). *Acta Cryst.* D**58**, 441–450.

Collaborative Computational Project, Number 4 (1994). *Acta Cryst.* D**50**, 760–763.

De Baere, I., Perutz, M. F., Kiger, L., Marden, M. C. & Poyart, C. (1994). *Proc. Natl Acad. Sci. USA*, **91**, 1594–1597.

De Jesús-Bonilla, W., Cruz, A., Lewis, A., Cerda, J., Barcelo, D. E., Cadilla, C. & López-Garriga, J. (2006). *J. Biol. Inorg. Chem.* **11**, 334–342.

De Jesús-Bonilla, W., Jia, Y., Alayash, A. & López-Garriga, J. (2007). *Biochemistry*, **46**, 10451–10460.

Dias, J. M., Bonifácio, C., Alves, T., Moura, J. J. G., Moura, I. & Romão, M. J. (2002). *Acta Cryst.* D**58**, 697–699.

Doyle, M. A., Vitali, J., Wittenberg, J. B., Vinogradov, S. N., Walz, D. A., Edwards, B. F. P. & Martin, P. D. (1994). *Acta Cryst.* D**50**, 757–759.

Garcia-Ruiz, J. M. (2003). *Methods Enzymol.* **368**, 130–154.

Gavira, J. A., Camara-Artigas, A., De Jesús, W., López-Garriga, J., Lewis, A., Yeh, S. & García-Ruiz, J. M. (2008). *J. Biol. Chem.* **283**, 9414–9423.

Gavira, J. A., de Jesus, W., Camara-Artigas, A., López-Garriga, J. & García-Ruiz, J. M. (2006). *Acta Cryst.* F**62**, 196–199.

Hockenhull-Johnson, J. D., Stern, M. S., Martin, P., Dass, C., Desiderio, D. M., Wittenberg, J. B., Vinogradov, S. N. & Walz, D. A. (1991). *J. Protein Chem.* **10**, 609–622.

Kemling, N., Kraus, D. W., Hockenhull-Johnson, J. D., Wittenberg, J. D., Vinogradov, S. N., Walz, D. A., Edwars, B. F. P. & Martin, P. (1991). *J. Mol. Biol.* **222**, 463–464.

Kimber, M. S. & Vallee, F. (2003). *Proteins*, **51**, 562–568.

Kraus, D. W. & Wittenberg, J. B. (1990). *J. Biol. Chem.* **265**, 16043–16053.

Mazzarella, L., Vergara, A., Vitagliano, L., Merlino, A., Bonomi, G., Scala, S., Verde, C. & di Prisco, G. (2006). *Proteins*, **65**, 490–498.

Mukai, M., Savard, P. Y., Ouellet, H., Guertin, M. & Yeh, S. R. (2002). *Biochemistry*, **41**, 3897–3905.

Murshudov, G. N., Vagin, A. A. & Dodson, E. J. (1997). *Acta Cryst.* D**53**, 240–255.

Otwinowski, Z. & Minor, W. (1997). *Methods Enzymol.* **276**, 307–326.

Ouellet, H., Juszczak, L., Dantsker, D., Samuni, U., Ouellet, Y., Savarad, P. Y., Wittenberg, J., Wittenberg, B., Friedman, J. M. & Guertin, M. (2003). *Biochemistry*, **42**, 5764–5774.

Peterson, E. S., Huang, S., Wang, J., Miller, M. L., Vidugiris, G., Kloek, A. P., Goldberg, D. E., Chance, M. R., Wittenberg, J. B. & Friedman, J. M. (1997). *Biochemistry*, **36**, 13110–13121.

Read, K. R. (1965). *Comp. Biochem. Physiol.* **15**, 137–157.

Robinson, V. L., Smith, B. B. & Arnone, A. (2003). *Biochemistry*, **42**, 10113–10125.

Ruiz-Martínez, C. R., Nieves-Marrero, C. A., Estremera-Andújar, R. A., Gavira, J. A., González-Ramírez, L. A., López-Garriga, J. & García-Ruiz, J. M. (2009). *Acta Cryst.* F**65**, 25–28.

Torres-Mercado, E., Renta, J. Y., Rodríguez, Y., López-Garriga, J. & Cadilla, C. L. (2003). *J. Protein Chem.* **22**, 683–690.

Vagin, A. & Teplyakov, A. (1997). *J. Appl. Cryst.* **30**, 1022–1025.

Vinogradov, S. N., Walz, D. A., Pohajdak, B., Mocns, L., Kapp, O. H., Suzuki, T. & Trotman, C. N. A. (1993). *Comp. Biochem. Physiol. B*, **106**, 1–26.

Yang, F. & Phillips, G. N. Jr (1996). *J. Mol. Biol.* **256**, 762–774.